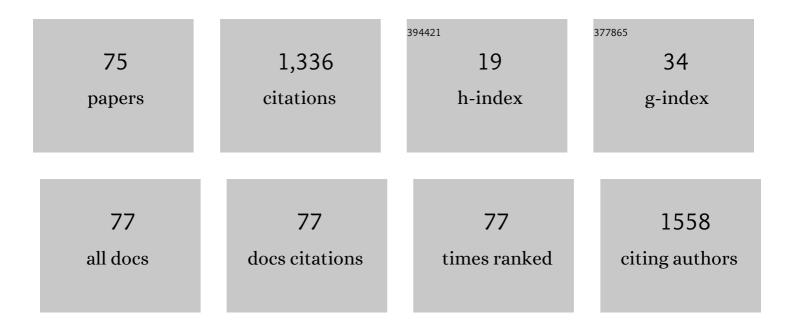
List of Publications by Year in descending order

Source: https://exaly.com/author-pdf/4501097/publications.pdf Version: 2024-02-01



YUNEELU

#	Article	lF	CITATIONS
1	Fabrication of TiO2 nanofibers/MXene Ti3C2 nanocomposites for photocatalytic H2 evolution by electrostatic self-assembly. Applied Surface Science, 2019, 496, 143647.	6.1	131
2	Enhanced energy-storage properties of 0.89Bi 0.5 Na 0.5 TiO 3 –0.06BaTiO 3 –0.05K 0.5 Na 0.5 NbO 3 lead-free anti-ferroelectric ceramics by two-step sintering method. Materials Letters, 2014, 114, 107-110.	2.6	127
3	Enhanced energy storage properties of BiAlO3 modified Bi0.5Na0.5TiO3–Bi0.5K0.5TiO3 lead-free antiferroelectric ceramics. Ceramics International, 2017, 43, 7653-7659.	4.8	123
4	Huge strain and energy storage density of A-site La3+ donor doped (Bi0.5Na0.5)0.94Ba0.06TiO3 ceramics. Ceramics International, 2017, 43, 106-110.	4.8	64
5	Synthesis and Photoluminescence of Assembly-Controlled ZnO Architectures by Aqueous Chemical Growth. Journal of Physical Chemistry C, 2009, 113, 1052-1059.	3.1	62
6	Hydrothermal synthesis of monosized Bi0.5Na0.5TiO3 spherical particles under low alkaline solution concentration. Journal of Alloys and Compounds, 2009, 484, 801-805.	5.5	50
7	Enhanced energy-storage properties of SrTiO3 doped (Bi1/2Na1/2)TiO3–(Bi1/2K1/2)TiO3 lead-free antiferroelectric ceramics. Journal of Materials Science: Materials in Electronics, 2014, 25, 4632-4637.	2.2	50
8	Porphyrinâ€based covalent triazine frameworks: Porosity, adsorption performance, and drug delivery. Journal of Polymer Science Part A, 2017, 55, 2594-2600.	2.3	50
9	Seed layer-free electrodeposition and characterization of vertically aligned ZnO nanorod array film. Journal of Solid State Electrochemistry, 2010, 14, 63-70.	2.5	38
10	Morphology-controlled synthesis, characterization, and luminescence properties of KEu(MoO4)2 microcrystals. CrystEngComm, 2013, 15, 2761.	2.6	37
11	Nanoscale origins of small hysteresis and remnant strain in Bi 0.5 Na 0.5 TiO 3 -based lead-free ceramics. Journal of the European Ceramic Society, 2017, 37, 3483-3491.	5.7	35
12	Rapid synthesis of Ni(OH) <sub>2</sub> /graphene nanosheets and NiO@Ni(OH) <sub>2</sub> /graphene nanosheets for supercapacitor applications. New Journal of Chemistry, 2019, 43, 3091-3098.	2.8	30
13	Enhanced energy storage properties of lead-free (1â^'x)Bi0.5Na0.5TiO3–xSrTiO3 antiferroelectric ceramics by two-step sintering method. Journal of Materials Science: Materials in Electronics, 2016, 27, 12479-12484.	2.2	27
14	Morphology and Photoluminescence of Ba <sub>0.5</sub> Sr <sub>0.5</sub> MoO <sub>4</sub> Powders by a Molten Salt Method. Journal of Nanomaterials, 2012, 2012, 1-6.	2.7	25
15	Optimized energy-storage performance in Mn-doped Na0.5Bi0.5TiO3-Sr0.7Bi0.2TiO3 lead-free dielectric thin films. Applied Surface Science, 2022, 571, 151274.	6.1	24
16	Facile synthesis of porous organic polymers bifunctionalized with azo and porphyrin groups. RSC Advances, 2015, 5, 98508-98513.	3.6	23
17	Hypercrosslinked conjugated microporous polymers for carbon capture and energy storage. New Journal of Chemistry, 2017, 41, 3915-3919.	2.8	23
18	Preparation and electrical properties of Ni0.6Mn2.4â^'Ti O4 NTC ceramics. Journal of Alloys and Compounds, 2015, 650, 931-935.	5.5	21

#	Article	IF	CITATIONS
19	Effects of sulfur substitution for oxygen on the thermoelectric properties of Bi2O2Se. Journal of the European Ceramic Society, 2020, 40, 5543-5548.	5.7	21
20	A slush-like polar structure for high energy storage performance in a Sr <sub>0.7</sub> Bi <sub>0.2</sub> TiO <sub>3</sub> lead-free relaxor ferroelectric thin film. Journal of Materials Chemistry A, 2022, 10, 7357-7365.	10.3	20
21	Large strain with low hysteresis in Sn-modified Bi0.5(Na0.75K0.25)0.5TiO3 lead-free piezoceramics. Journal of Materials Science, 2020, 55, 1388-1398.	3.7	19
22	Preparation routes and electrical properties for Ni0.6Mn2.4O4 NTC ceramics. Journal of Materials Science: Materials in Electronics, 2015, 26, 7238-7243.	2.2	18
23	Enhanced strains of Nb-doped BNKT-4ST piezoelectric ceramics via phase boundary and domain design. Ceramics International, 2021, 47, 24207-24217.	4.8	17
24	Multiple morphologies of YF 3 : Eu 3+ microcrystals: Microwave hydrothemal synthesis, growth mechanism and luminescence properties. Ceramics International, 2016, 42, 1513-1520.	4.8	16
25	Nitrogen-rich hierarchical porous carbon supported Ag nanoparticles for efficient nitrophenol reduction. Microporous and Mesoporous Materials, 2019, 290, 109672.	4.4	16
26	Evolution of mineral phases and microstructure of high efficiency Si–Ca–K–Mg fertilizer prepared by water-insoluble K-feldspar. Journal of Sol-Gel Science and Technology, 2020, 94, 3-10.	2.4	14
27	Highly uniform NaLa(MoO4)2:Eu3+ microspheres: microwave-assisted hydrothermal synthesis, growth mechanism and enhanced luminescent properties. Journal of Materials Science: Materials in Electronics, 2014, 25, 3109-3115.	2.2	13
28	Structure and dielectric properties of Nd substituted Bi1.5MgNb1.5O7 ceramics. Journal of Materials Science: Materials in Electronics, 2013, 24, 2785-2789.	2.2	11
29	Realizing white emission in Sc2(MoO4)3:Eu3+/Dy3+/Ce3+ phosphors through computation and experiment. Journal of Solid State Chemistry, 2020, 290, 121592.	2.9	11
30	<i>De novo</i> fabrication of multi-heteroatom-doped carbonaceous materials <i>via</i> an <i>in situ</i> doping strategy. Journal of Materials Chemistry A, 2020, 8, 4740-4746.	10.3	11
31	Porphyrin-based covalent triazine framework and its carbonized derivative as catalyst scaffold of Au and Ag nanoparticles for 4-nitrophenol reduction. Microporous and Mesoporous Materials, 2022, 330, 111611.	4.4	11
32	Preparation and characterization of Ni0.6Mn2.4O4 NTC ceramics by solid-state coordination reaction. Journal of Materials Science: Materials in Electronics, 2013, 24, 5183-5188.	2.2	10
33	Giant strain response with low hysteresis in potassium sodium niobate based lead-free ceramics. Ceramics International, 2019, 45, 14675-14683.	4.8	10
34	Robust perfluorinated porous organic networks: Succinct synthetic strategy and application in chlorofluorocarbons adsorption. Nano Research, 2021, 14, 3282-3287.	10.4	9
35	Microwave hydro/solvothermal synthesis of octahedron-like NaEu(MoO4)2 microarchitectures by EDTA-assisted and photoluminescence property. Journal of Materials Science: Materials in Electronics, 2014, 25, 2359-2365.	2.2	8
36	Molten salt synthesis and tunable photoluminescent properties of Eu3+–Tb3+ doped NaY(MoO4)2 microcrystals. Journal of Materials Science: Materials in Electronics, 2015, 26, 2987-2994.	2.2	8

#	Article	IF	CITATIONS
37	Enhanced strains by flexible nanoscale domain structure in BNKT-SBT relaxor ferroelectrics. Journal of Materials Chemistry C, 2022, 10, 9628-9635.	5.5	8
38	Impact of Ni dopant on structure and electrical properties of PMN-0.1PT ceramics. Journal of Materials Science: Materials in Electronics, 2017, 28, 7525-7531.	2.2	7
39	Grain size engineering and growth mechanism in hydrothermal synthesis of Bi0.5Na0.5TiO3 thin films on Nb-doped SrTiO3 substrates. Journal of Sol-Gel Science and Technology, 2021, 99, 366-375.	2.4	7
40	Morphology and photoluminescence properties of KSm(MoO4)2 microcrystals by a molten salt method. Journal of Materials Science: Materials in Electronics, 2014, 25, 3608-3613.	2.2	6
41	Regulated morphology of ScF3: Eu3+, Bi3+ microcrystals: Microwave-assisted hydrothermal synthesis, structure and luminescence properties. Journal of Solid State Chemistry, 2019, 269, 447-453.	2.9	6
42	Enhanced Electrostrictive Coefficient and Suppressive Hysteresis in Lead-Free Ba(1â^'x)SrxTiO3 Piezoelectric Ceramics with High Strain. Crystals, 2021, 11, 555.	2.2	6
43	Structure and electric properties of (1â^'x)(Bi1/2Na1/2) TiO3-xBaTiO3 Systems. Journal Wuhan University of Technology, Materials Science Edition, 2007, 22, 315-319.	1.0	5
44	Growth of Bi1.5MgNb1.5O7 thin films on Pt/Ti/SiO2/Si substrates by RF magnetron sputtering. Journal of Materials Science: Materials in Electronics, 2014, 25, 1474-1479.	2.2	5
45	Morphology and photoluminescent properties of KLa(MoO4)2 (doped with Eu3+) synthesized by a molten salt method. Journal of Materials Science: Materials in Electronics, 2016, 27, 10473-10478.	2.2	5
46	Enhanced large field-induced strain and energy storage properties of Sr0.6La0.2Ba0.1TiO3-modified Bi0.5Na0.5TiO3 relaxor ceramics. Journal of Materials Science: Materials in Electronics, 2022, 33, 15779-15790.	2.2	5
47	Citric acid-mediated microwave-assisted hydrothermal synthesis and luminescence property of NaSm(MoO4)2 submicro-crystals. Journal of Materials Science: Materials in Electronics, 2015, 26, 8595-8602.	2.2	4
48	TEM study of incommensurate superstructure in Pb1â^'0.5xNbx((Zr0.52Sn0.48)0.955Ti0.045)1â^'xO3 ceramics with 0–1 switching characteristic strain and high energy storage density. Journal of Materials Science: Materials in Electronics, 2019, 30, 12375-12381.	2.2	4
49	Improved strain and low hysteresis in (0.9-x)BaTiO3-xCaTiO3-0.1Ba(Zr0.7Sn0.3)O3 lead-free relaxor ferroelectrics. Ceramics International, 2020, 46, 24231-24237.	4.8	4
50	Synthesis of carbazole-based polymer derived N-enriched porous carbon for dyes sorption. Polymer Bulletin, 2021, 78, 3311-3325.	3.3	4
51	Ferroelectric–relaxor phase evolution and enhanced electromechanical strain response in LaAlO3-modified Bi0.5Na0.5TiO3–Bi0.5K0.5TiO3 lead-free ceramics. Journal of Materials Science: Materials in Electronics, 2021, 32, 28436-28446.	2.2	4
52	Heteroepitaxial Growth of 1T MoS 2 Nanosheets on SnO 2 with Synergetic Improvement on Photocatalytic Activity. Crystal Research and Technology, 2021, 56, 2000091.	1.3	4
53	Sputtering pressure dependent composition and dielectric properties in Bi1.5MgNb1.5O7 thin films deposited at room temperature by RF magnetron sputtering. Journal of Materials Science: Materials in Electronics, 2013, 24, 5085-5090.	2.2	3
54	MICROWAVE-ASSISTED HYDROTHERMAL SYNTHESIS AND LUMINESCENCE PROPERTIES OF <font>Eu</font> <sup>3+</sup> -DOPED <font>CdTe</font> QUANTUM DOTS. Nano, 2014, 09, 1450044.	1.0	3

#	Article	IF	CITATIONS
55	Microwave-assisted hydrothermal synthesis and photoluminescence property of NaSm(MoO4)2 octahedral crystals. Journal of Materials Science: Materials in Electronics, 2015, 26, 3926-3932.	2.2	3
56	Investigation of Multiply Twins in Mn <sub>2.02</sub> Co <sub>0.98</sub> O <sub>4</sub> Ceramic by Means of Transmission Electron Microscopy. Journal of the American Ceramic Society, 2016, 99, 3458-3466.	3.8	3
57	A nanoscale porous glucose-based polymer for gas adsorption and drug delivery. New Journal of Chemistry, 2018, 42, 15692-15697.	2.8	3
58	Microwave hydrothermal synthesis, annealing and luminescence properties of BaWO4:3%Eu3+ microcrystals. Journal of Materials Science: Materials in Electronics, 2019, 30, 14190-14199.	2.2	3
59	Large strain response and fatigue-resistant behavior of lead-free (1-x)(Bi <sub>0.5</sub> Na <sub>0.5</sub> )TiO <sub>3</sub> - <i>x</i> SrTiO <sub>3</sub> ceramics at a relatively low driving field. Materials Research Express, 2019, 6, 115218.	1.6	3
60	Co3O4 nanocrystals grown on graphene nanosheets for high-performance supercapacitor with excellent rate capability. Journal of Sol-Gel Science and Technology, 2019, 89, 634-640.	2.4	3
61	Elucidating the electronic structures and photoluminescence properties of single-phase ScF3:Dy3+, Eu3+, Ce3+ phosphors for LEDs. Journal of Sol-Gel Science and Technology, 2020, 96, 753-762.	2.4	3
62	Electronic structure, morphology-controlled synthesis, and luminescence properties of YF3: Eu3+. Journal of Sol-Gel Science and Technology, 2021, 98, 497-507.	2.4	3
63	Enhanced electrical properties of the polymorphic phase boundary on the tetragonal side in K0.48Na0.52NbO3-based lead-free piezoelectric ceramics. Ceramics International, 2022, 48, 17246-17252.	4.8	3
64	Using layer-by-layer assembly to fabricate NaLa(MoO4)2@CdTe core–shell microspheres with high fluorescence. Journal of Materials Science, 2014, 49, 4506-4512.	3.7	2
65	Morphology and photoluminescence properties of NaNd(MoO4)2 synthesized by a molten salt method. Journal of Materials Science: Materials in Electronics, 2016, 27, 5735-5740.	2.2	2
66	Phase transition and huge field-induced strain of BaZrO3 modified (Bi0.5Na0.5)0.94Ba0.06TiO3 ceramics. Journal of Materials Science: Materials in Electronics, 2017, 28, 14664-14671.	2.2	2
67	Easy-to-use model to reveal the nature of octahedral rotation transformations in perovskites. Ceramics International, 2020, 46, 4477-4483.	4.8	2
68	The formation process of aluminum hydroxide in calcium sulfoaluminate pastes. Chemical Papers, 2021, 75, 909-920.	2.2	2
69	High strain response and low hysteresis in BaZrO3-modified KNN-based lead-free relaxor ceramics. Journal of Materials Science: Materials in Electronics, 2021, 32, 16715-16725.	2.2	2
70	Large strain and low hysteresis in (1-x)Bi0.5(Na0.75K0.25)0.5TiO3-xSrTiO3 lead-free piezoceramics. Materials Research Express, 2021, 8, 056303.	1.6	2
71	Orientation dependent intrinsic and extrinsic contributions to the piezoelectric response in lead-free (Na0.5K0.5)NbO3 based films. Journal of Alloys and Compounds, 2022, 906, 164346.	5.5	2
72	Citric sol–gel synthesis and luminescence characteristics of Ca1â^'y Sr y La2â^'x Eu x ZnO5 phosphors. Journal of Materials Science: Materials in Electronics, 2015, 26, 5618-5624.	2.2	1

#	Article	IF	CITATIONS
73	Preparation and electrical properties of Pb(1–1.5x)Lax(Zr0.66Sn0.25Ti0.09)O3 ceramics. Journal of Materials Science: Materials in Electronics, 2017, 28, 15953-15958.	2.2	1
74	Enhanced photoluminescence property of KLa1â^'xEux(MoO4)2 with concentration gradient. Journal of Materials Science: Materials in Electronics, 2017, 28, 4941-4945.	2.2	0
75	Erratum to "Nanoscale origins of small hysteresis and remnant strain in Bi0.5Na0.5TiO3-based lead-free ceramics―[Journal of the European Ceramic Society 37/11 (2017) 3483–3491]. Journal of the European Ceramic Society, 2018, 38, 359.	5.7	0